Forensic Science International 303 (2019) 109934

Contents lists available at ScienceDirect

Forensic Science International

journal homepage: www.elsevier.com/locate/forsciint

Experimental and theoretical studies into the release of blood droplets from weapon tips

Craig D. Adam

School of Chemical and Physical Sciences, Lennard-Jones Laboratories, Keele University, Keele, Staffordshire ST5 5BG, UK

ARTICLE INFO

Article history:
Received 4 May 2019
Received in revised form 13 August 2019
Accepted 19 August 2019
Available online 22 August 2019

Keywords:
Forensic
Bloodstain pattern analysis
Blood spatter
Blood droplet
Swing cast-off
Surface tension

ABSTRACT

The formation and release under gravity of blood droplets from simulated weapon tips has been investigated experimentally and the results analysed and interpreted using established theoretical models for detached pendent drops. Droplets were produced from a series of conical nozzles, manufactured with a range of cone angles and including a set of un-bored conical tips, under conditions where the tip was either non-wetted or pre-wetted with blood. For the former, radius-limited case, detached droplet volumes were found to agree well with the predictions of both the pendent drop weight and drop shape models. For pre-wetted tips, droplet volumes were found to increase with increasing cone angle and to be independent of whether the blood flow was through an orifice at the tip or across the tip surface itself for un-bored tips. Such angle-limited, detached droplet volumes were predicted well by applying the same contact angle correction factor as for a flat surface. The maximum droplet volume, formed from a horizontal flat surface, was found to be around 150 μL for horse blood. Similar theoretical approaches were then extended to droplets released under centrifugal force appropriate to swing cast-off activity and evaluated using previously published experimental data. Order of magnitude agreement for droplet diameters was fairly good but, more importantly, these were found to be proportional to the inverse of the tangential velocity thereby supporting a model where the blood droplet is released directly from a blood mass itself, such as a ligament, rather than from being pinned to some surface feature or orifice on the weapon. This work provides a sound theoretical and experimental understanding of blood droplet release under these conditions that can underpin both future research and the interpretation of blood evidence in case-work.

1. Introduction

Over recent years there have been many published studies exploring the science underpinning bloodstain pattern analysis. Amongst this literature, many of these [1–9] have focused on the dynamics of blood droplets, surface impact and stain formation, including impact angle and surface texture effects, whilst others have investigated pattern formation itself, for example by analysing droplet trajectories and the methodologies used in case-work examination and interpretation [10–15]. In contrast, there are fewer examples where the initial formation of the blood droplets themselves has been studied, for example on weapon tips, and specifically the factors which govern the volume of the droplet released whether under passive (drip from a static source) or active (for example, from swing cast-off) conditions [16–18]. Studies of these factors, for the most part, have focused on experimental investigations rather than exploration of the theoretical basis for droplet formation and the verification of such mathematical models against those experimental data.

This present work was designed to fill this gap in the literature by reviewing and developing current understanding of the mechanisms underpinning the formation and adhesion of blood droplets at orifices and on surfaces – the pendent drop – and the conditions under which droplets are released, either under gravity alone or under the centrifugal force generated during swing cast-off. To test and evaluate such a quantitative, theoretical approach, a series of experiments was carried out to obtain data on the relationship between the size, shape and properties of the orifice or surface and the volume of blood droplets formed on passive release. This was achieved by using bored and un-bored conical brass tips machined at a variety of angles as models for weapon tips of differing sharpness. In this study particular attention was paid to the degree of wetting of the surface by the blood and the consequent size of the detached droplet. In addition, quantitative data already published, from model swing cast-off studies [12,16], has been used in a similar fashion to evaluate mathematical models for the active release of blood droplets.

E-mail address: c.d.adam@keele.ac.uk (C.D. Adam).

http://dx.doi.org/10.1016/j.forsciint.2019.109934
0379-0738/

Although casework applications relate almost exclusively to human blood, blood droplets and bloodstains, in the research context other sources of blood are frequently used [1–18]. In addition to many examples of the use of porcine blood in blood dynamics studies, more recently, defibrinated horse blood has been utilised due to its commercial availability. In this present work, the experimental data and its interpretation are carried out in the context of horse blood while, in explaining the theoretical aspects and in discussions, comparison with human blood and, where appropriate, porcine blood are made.

2. Theory of droplet formation

Although the basic physical principles underpinning the formation of a pendent drop and its subsequent release are fairly straightforward, there are several modifications and refinements of this theory that are necessary to obtain mathematical models that fully support experimental findings. In this section, these will be reviewed with a view to focusing on those aspects which are of direct use in providing an understanding of benefit to the context of forensic blood evidence. A good introduction and overview of much of the basic fluid dynamics theory is provided by Middleman [19].

2.1. The balance of forces approach and the drop-weight method

Historically, the need for a detailed understanding of the pendent drop arose through it being the basis of methods for the determination of the surface tension of a liquid. Hence, Tate's Law was formulated [19] which balances the weight of the pendent drop against the surface tension force around the interface between the neck of the liquid and the orifice supplying it. As the drop grows in size there will be a maximum weight that can be supported by the finite surface tension force, at which point the drop detaches from the orifice. As the size of the droplet detached in this fashion is determined by the size of the orifice, such droplets are termed 'radius-limited'.

It was realised many years ago [20,21] that the volume of the detached droplet is in fact less than that of the maximum pendent drop volume since the fracture point occurs across the neck region of the liquid that forms in the final stages before detachment, rather than at the junction with the orifice itself. Consequently an empirical correction factor was suggested by Rayleigh [20] which was later refined by Harkins and Brown [21] to become the theoretical basis of an acknowledged standard method for surface tension measurement — the 'drop-weight method'. Although originally provided as a curve defined by discrete experimental data points, there have been several attempts to fit analytical functions to this correction factor so providing a more convenient form for the user [22–24]. More recently an equivalent correction curve has been derived from theoretical considerations and provided with a simple analytical form [25]. In all these cases only the lower section of the curve has been studied.

It is important to reflect on some of the detailed assumptions built into this model when wishing to extrapolate it to the wider range of scenarios appropriate to blood droplet formation. For an orifice of radius R and a liquid of density ρ and surface tension γ, we may balance the forces as:

$$2\pi R\gamma\cos\theta = \rho g V_p \tag{1}$$

Here V_p is the volume of the pendent drop and θ is the contact angle between the liquid surface and the thin wall of the orifice around the, assumed circular, contact line between liquid and orifice. The maximum stable drop volume will be found when the surface tension force is at a maximum. This occurs when the contact angle is zero which requires the liquid surface to neck from the pendent drop towards the orifice. Hence, we can write Tate's Law as:

$$V_p = \pi a^{*2} R \tag{2}$$

where $a^* = \sqrt{2\gamma/\rho g}$ is defined as the capillary length for the liquid. Note that this constant is sometimes defined alternatively without the factor of 2 in the expression. Using appropriate values of γ and ρ for human blood [6], the capillary length for human blood may be evaluated as:

$$a^* = \sqrt{\frac{2 \times 0.062}{1060 \times 9.81}} = 3.453 \times 10^{-3}\text{m}$$

To obtain the detached droplet volume V, we need to include the empirical Harkins and Brown correction factor F, [20] to Tate's Law, to get:

$$V = \pi a^{*2} R F\left(\frac{R}{V^{1/3}}\right) \tag{3}$$

The H–B correction factor is tabulated normally as a function of $R/V^{1/3}$ and less commonly in terms of R/a^*. For small orifices the function F approaches unity from below as $R/V^{1/3}$ tends to zero, while, as $R/V^{1/3}$ increases, the correction factor decreases towards a minimum of ~0.6 at $R/V^{1/3}$ ~0.85 before rising to around 0.65 and then finally dropping away again as $R/V^{1/3}$ becomes greater than ~1.5. Using Eq. (3), the surface tension of a liquid may be calculated by measuring the volume/mass of the detached spherical droplet for a known orifice size.

In the context of blood droplet formation, this idealised cylindrical orifice is of limited use as blood may drip from wounds of all shapes and sizes or from weapons, body surfaces or other items at the crime scene where the blood directly gathers on the surface before a pendent drop is formed at some appropriate point. Droplet formation on the underside of a solid surface is theoretically similar to the dripping that takes place from an orifice of sufficiently large diameter such that the pendent droplet reaches its maximum volume before it is able to pin itself to the circumference of the orifice itself. In these cases the pendent drop formation is said to be 'angle-limited' rather than 'radius-limited' since the liquid surface on the droplet runs continuously into the liquid surface at the large orifice or, equivalently, on to the solid surface itself.

The important consequence for these cases is that the pendent drop volume will depend on the contact angle with the surface of the solid material or the liquid at the mouth of the orifice itself. In the former case, the wetting ability of the liquid on that surface is critical while in the latter case the expectation is that the drop surface will spread outwards, rather than neck inwards, to achieve zero contact angle and hence maximum surface tension support for the pendent drop. It should also be noted that even when the drop is pinned to the mouth of a small orifice, the thickness of the orifice wall and the hydrophobic/hydrophilic nature of the material from which it is made will determine whether the pining occurs to the inside wall (the hydrophobic case) or to the outside wall (the hydrophilic case).

The largest pendent drops will occur in angle-limited situations and, for the case of a zero contact angle, the detached droplet will have the maximum possible volume for a free liquid droplet. An estimate of this 'maximum droplet volume' was provided by Campbell [26] in the context of condensing metal vapours on solid electrodes. Here it was assumed that the threshold for the detaching droplet occurs when the pendent drop forms a hemispherical shape tethered to the surface by a liquid bridge that meets the surface at zero contact angle. Since the hemispherical volume reforms into a spherical droplet shortly after

detachment, Campbell's resulting formula applied to human blood (using a* given previously) provides an estimate of the diameter d of this spherical droplet of maximum volume, given by:

$$d = 2^{2/3}\sqrt{\frac{3\gamma}{\rho g}} = 1.944 \times a^{*} = 6.71\text{mm} \quad (4)$$

This corresponds to a maximum detached droplet volume of 158 μL for human blood.

2.2. The calculation of the droplet profile — the pendent drop method

To overcome the difficulties in dealing with the H–B correction, an alternative approach was developed based on calculating the profile of pendent drop under the combined forces of gravity, surface tension and the pressure difference across the drop surface using the axisymmetric solution of the Young–Laplace equation [27]. Thus, not only could the theoretical profile shapes be compared with those observed experimentally for the pendent drop prior to detachment, but the profile for maximum volume could be calculated as well. However, until numerical solutions of the differential equation using digital computers became available from the 1970s, the applicability and detail that could be drawn from these calculations were limited. Nevertheless, novel situations such as the formation of pendent drops on conical tips [28] were tackled using this method.

Following on from work on radius-limited pendent droplets [29,30], a detailed study of both radius and angle-limited drops was reported [31] and later investigated in greater detail [32,33]. These latter studies include tabulated data on radius-limited detached droplets as well as the variation in maximum pendent droplet volume as a function of contact angle on flat horizontal surfaces. The relationship between surface shape and droplet formation has been studied to a much lesser extent. Most notably, pendent drops on solid conical tips have been the subject of droplet profile calculations based on the Laplace method, on the basis of a zero contact angle with the tip surface [34]. Parallel experimental studies were undertaken using what were regarded as 'perfectly wetting' liquids [35].

2.3. Prediction of detached droplet volumes

Building on these theoretical developments, some of the calculations most relevant to the current work will now be discussed. First the approach developed here for the prediction of detached droplet volumes from an orifice will be presented.

Eq. (3) was devised originally for the calculation of the surface tension of a liquid from measurements of the detached droplet volume V. As such, the H–B correction function F is calculated using the measured value for V. In this current work, it is the prediction of V itself that is of interest and its comparison with that measured experimentally so Eq. (3) cannot be used directly. Consequently, an alternative method for deducing the appropriate correction factor was needed. This was based on an iterative calculation where the uncorrected volume was used as an initial estimate of the true detached volume in the calculation of F, leading to a calculation of a fresh estimate of V which is closer to the true value. This process was continued using the new estimate to re-calculate the correction factor until applying a further iteration did not significantly change the value of the detached volume. The so-called convergence criterion was taken to be when the volume remains unchanged to four significant figures.

To generate these corrected volumes, Eq. (3) may be written in iterative form as:

$$V_{n+1} = \pi a^{*2} R F\left(\frac{R}{V_n^{1/3}}\right) \quad (5)$$

where $V_1 = \pi a^{*2} R$ and n specifies the number of the iteration. The relevant detached droplet volume V was calculated by incorporating the appropriate value of F. It was found that the iteration converged well, within two to six iterations, to a final value of V, by using the uncorrected volume V_1 as the first estimate. To calculate F at each iterative step, the tabulated values of the function [23] were preferred to the analytical form [25], partly as they extended to larger values of the abscissa and partly as they more accurately represented the original, experimentally-derived form of the function [21]. Simple linear interpolation was used to determine intermediate values where needed. It has been shown that for large values of the abscissa the function F is inversely proportional to $R/V^{1/3}$ [26]. This approach was used to extend F from $R/V^{1/3} = 1.59$ up to $R/V^{1/3} = 2.35$ and, by matching this section to the final few points of the tabulated data [23], the constant of proportionality was determined. This gave the form of F over this range as:

$$F \approx \frac{0.855}{\left(R/V^{1/3}\right)} \quad (6)$$

The constant derived here (0.855) is very close to the value of 0.845 estimated in reference [26] where a graphical figure showing the form of F over the full range is also provided.

Using the appropriate values of γ/ρ given in Section 3, the variation of detached droplet volume as a function of orifice diameter for both water and for the defibrinated horse blood used later in this work, is shown in Fig. 1. The difference in volumes for the two liquids is due mainly to the larger surface tension constant for water. In both cases the droplet volume increases monotonically with orifice diameter in an approximately linear fashion. This represents the formation of radius-limited droplets. Eventually, the liquid ceases to pin on to the orifice wall and instead contacts directly with the surrounding liquid surface at zero contact angle to form an angle-dependent droplet whose detached volume is independent of the orifice size. This represents the formation of droplets of maximum volume from an orifice. The predictions in Fig. 1 show that, for horse blood, this threshold occurs at around 16 mm contact diameter, with a detached droplet volume of 205 μL.

3. Materials and methods

The basic experimental technique for producing blood droplets from orifice tips is fairly straightforward though care needs to be taken at various points to ensure the reproducibility of results. Defibrinated horse blood was obtained from TCS Biosciences Ltd.,

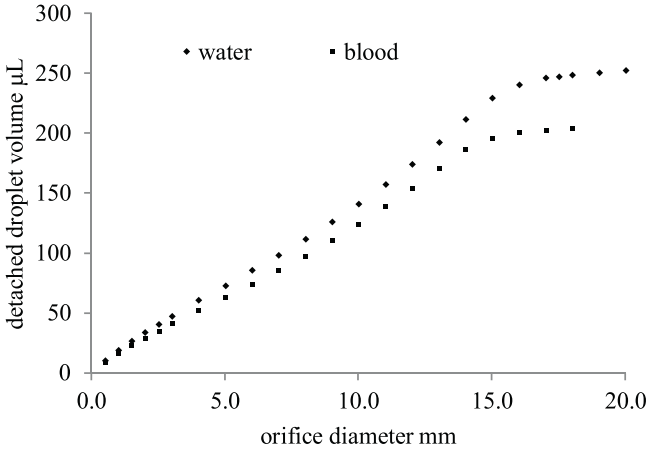

Fig. 1. Detached droplet volume under radius-limited conditions as a function of orifice diameter (drop weight theory).

Buckingham, UK and stored in a refrigerator. This material has been shown to be suitable alternative to human blood for blood dynamics and pattern analysis research and retains its properties for up to twelve days of storage [36]. All samples were agitated and brought to room temperature before use. Each sample was used for only a short period before a fresh amount of blood was taken from the refrigerator. These procedures were found to produce consistent results.

A glass separating funnel fitted with a tap acted as a reservoir for the blood and was secured to a Kaiser *rePro* photographic camera (copy) stand. A tapered, plastic nozzle (tip diameter ~0.5 mm) fitted to the reservoir allowed for the easy attachment of the relevant bored brass nozzle. For the un-bored nozzles, a short piece of flexible polythene hose was used to link the reservoir to the plastic nozzle which was then held in position against the brass nozzle tip to generate the formation of angle-limited blood droplets from that nozzle surface. Droplets could be produced reliably and at a defined rate by careful control of the tap.

Sets of nozzles were manufactured from cylindrical brass rod that were machined into a conical shape at one end with cone angles of 30°, 60°, 90°, 120°, 150° and 180° degrees — this last corresponding to a flat surface. One of the sets was un-bored while the other sets had holes of 1 mm, 2 mm or 3 mm diameter bored along the symmetry axis to produce a nozzle tip that had an orifice of known diameter with conical edges at the specified angle. A full set of angles with the 2 mm bore was produced while the 1 mm bore was restricted to the smaller angles – 30° and 60° while the 3 mm bore corresponded to the larger angles – 90°, 120°, 150° and 180°. In total 18 nozzles were manufactured. The inner nozzle diameters were measured using a low powered microscope with calibrated graticule and found to be equal to or a very little less than the designed diameter; those measured values are given in Table 1.

Using the twelve bored nozzles, radius-limited droplets were formed by ensuring that the blood was not allowed to wet the conical nozzle surface around the tip while, in separate experiments, angle-limited droplets were formed by pre-wetting the tip area with blood. Another set of measurements using demineralised water produced corresponding radius-limited droplets, these results being used for calibration and comparison purposes. Droplet formation on the un-bored nozzles was subject to pre-wetting of the nozzle surface with blood and careful adjustment of the plastic nozzle that was delivering the blood from the reservoir.

Imaging of selected droplets on each tip was carried out using a Motic digital camera and images were analysed with Motic Images Plus 2.0 imaging and analysis software. Examples of the droplet images produced on wetted nozzles are shown in Fig. 2. Droplets were counted and their drop rate measured automatically using an optical gate linked to a Pasco measurement system. Droplet volumes were obtained gravimetrically from an accumulation of between ten and fifty droplets, ensuring that for all measurements a weight of at least 0.5 g was recorded to four decimal places. Droplet formation rates of around one per minute were adopted. It has been suggested that the optimum rate should be no faster than one drop every three minutes [21] but such formation times were found to lead to physical changes to the blood itself, in and around the tip, which led to poor reproducibility. Each measurement was taken at least three times and a mean value calculated. Contact angles were measured on the images using a tool within the Motic software.

All measurements were stored within Excel spreadsheets where all the data processing and analysis was carried out. Both the surface tension and density of the blood are relevant to the analysis of the results. As is evident from Eq. (3), the detached droplet volume depends on the constant a^* which is a function of the ratio of γ/ρ. Further, since the H–B correction factor F is independent of the properties of the liquid, it has been shown [28,32] that, for the same conical tip, the ratio of the radius-limited droplet volumes from two different liquids – say, blood (V_b) and water (V_w) – follow from Eq. (3), giving:

$$\frac{V_b}{V_w} = \left(\frac{\gamma_b \rho_w}{\gamma_w \rho_b}\right)^{3/2} \tag{7}$$

This relationship continues to apply to angle-limited droplets if the contact angles for the two liquids are the same. It follows that the distinct values of ρ_b and γ_b are not needed to interpret these results, only the ratio of these quantities and that may be calculated from data obtained through a series of similar measurements of droplet volume performed using blood and water, for which both parameters are known with some precision.

Using the set of results for radius-limited droplets, to be described in the following section (Table 1), together with the density ($\rho = 998$ kg m^{-3}) and surface tension ($\gamma = 0.0728$ N m^{-1}) for

Table 1
Drop volume results for water and horse blood for non-wetted nozzles.

Nozzle diameter $2R$ mm	Nozzle cone angle deg	Water		Horse blood	
		Drop volume V_w μL	Standard error μL	Drop volume V_b μL	Standard error μL
1.00	Theory[a]	19.1	–	16.4	–
0.99	30	20.1	0.1	16.3	0.3
0.99	60	20.3	0.1	15.5	[b]
2.00	Theory[a]	33.9	–	29.2	–
1.96	30	34.0	0.4	29.1	0.3
1.94	60	34.0	0.4	29.7	1.0
1.98	90	36.2	0.2	29.6	0.4
2.00	120	38.4	0.4	30.5	0.2
2.02	150	41.2	0.4	31.4	0.5
1.98	180	36.4	0.2	29.2	0.1
3.00	Theory[a]	47.5	–	41.0	–
2.99	90	49.7	0.3	40.0	0.4
2.94	120	51.9	0.2	42.6	0.5
2.99	150	53.9	0.9	42.8	0.7
2.94	180	55.2	0.6	47.1	1.0

[a] Calculated from Eq. (3) as described in the text.
[b] Only a single measurement was made due to accidental damage to the nozzle.

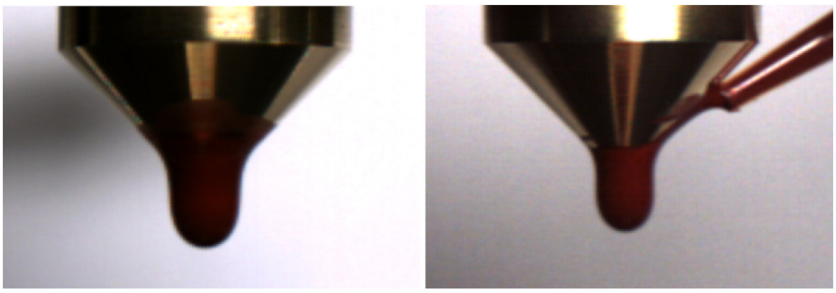

(a) (b)

Fig. 2. Droplet formation on wetted 90° conical nozzles; (a) 3 mm orifice (b) non-bored cone.

demineralised water at 20 °C [37], the mean ratio for defibrinated horse blood was calculated as:

$$\frac{\gamma_b}{\rho_b} = 6.35 \pm 0.05 \times 10^{-5} \mathrm{m}^{-3}\mathrm{s}^{-2}$$

where the uncertainty is quoted as the standard error. Taking the density of horse blood as 1050 kg m^{-3} [36], this result gives the surface tension of the blood, under the conditions of these experiments, as 0.0667 N m^{-1}; this appears to be in line with values for surface tension for blood from other mammalian species. It should be emphasised that in the calculations throughout this work it is this ratio that is utilised in calculations rather than the individual values of these two properties. The capillary length for horse blood, derived from this ratio and used in subsequent calculations, is $a^* = 3.598 \times 10^{-3}$m.

4. Results

4.1. Radius-limited droplets: non-wetted nozzles

The detached droplet volumes from the conical nozzles, for both water and blood, where the liquid was not allowed to wet the nozzle tip prior to droplet formation, are given in Table 1. The volumes predicted for each nozzle diameter according to the drop weight theory (Sections 2.1 and 2.3) incorporating the H–B correction (Eq. (3)), are included here for comparison. It is clear that, for each nozzle, the detached volumes for horse blood are all less than those for water due to the higher surface tension for the latter liquid. For the most acute cone angles the detached volumes for both liquids are very close to those predicted theoretically. Across all cone angles these volumes remain close to the theoretical values but are on average a little larger for the more obtuse angles and the widest nozzle diameter as these conditions tend to encourage slight wetting by the liquid. Since faster drop rates lead to an increase in the detached droplet volume [21] it is also possible that working here with a rate of around one drop per minute rather than one every three minutes or more has contributed to these experimental volumes being generally larger than the theoretical values. Comparison between the droplet volumes for the two liquids suggests that it is probable that some of the scatter in these values, outside of the standard error, may be attributed to microscopic imperfections in each nozzle arising from the machining process during manufacture.

4.2. Angle-limited droplets: wetted nozzles

The experimental detached droplet volumes where the nozzle tip was pre-wetted with blood prior to formation of the droplet, are given in Table 2. These include outcomes from the non-bored cone tips where the pendent droplet was allowed to form slowly by blood flowing across the cone surface. Uncertainties are included here again as standard errors. Note that these appear consistently larger for the 150° and particularly the 180° tips, than for the smaller cone angles. It is suggested that this is due to difficulties in ensuring a consistent and uniform pre-wetting of the tips and, for these large cone angles, a longer contact line between the pendant droplet and the tip and a greater area of wetting. These factors lead to more variation in the net surface tension force acting to hold the growing droplet in place and hence more variation in the consequent detached droplet volume between repeat measurements.

There are three principal conclusions to be drawn from these results. Firstly, the pre-wetting allows much larger, angle-limited pendent droplets to accumulate on a tip and the volume increases significantly with increasing cone angle. Secondly, for the 30° tips, these detached droplet volumes are only a little larger than those found for the non-wetted tips of the same cone angle (Table 1) with that for the non-bored tip being the smallest and the others increasing slightly with nozzle diameter. Finally, although there is some scatter in the values, detached droplet volumes from a given cone angle are generally independent of orifice diameter, including those from the non-bored tips. In other words the volume, for a given cone angle, is the same whether it was formed on a bored or non-bored tip. The slightly lower volume obtained for the

Table 2
Drop volume results for horse blood for wetted bored and non-bored cone tips.

Nozzle diameter $2R$ mm	Nozzle cone angle deg	Horse blood	
		Drop volume V μL	Standard error μL
0.99	30	30.5	1.6
0.99	60	47.6	0.4
1.96	30	34.1	0.6
1.94	60	48.2	0.7
1.98	90	63.5	1.3
2.00	120	85.3	0.7
2.02	150	112	4
1.98	180	157	5
2.99	90	65.3	0.8
2.94	120	87.4	1.0
2.99	150	107	1
2.94	180	154	6
Non-bored cone tips	30	28.4	0.3
	60	45.6	0.9
	90	62.5	1.4
	120	85.5	1.5
	150	116	2
	180	138	3

non-bored 180° tip may be due to the experimental difficulties in facilitating the flow of blood on to the underside surface under those conditions. The outcomes for the 180° tips show a maximum detached droplet volume of order 150 μL. These results are displayed graphically as a function of cone angle in Fig. 4. This figure includes comparison with theoretical values and will be discussed in Section 5.2.

5. Discussion

Next, the principal consequences of these results will be discussed which, for convenience, may be separated into three areas. Firstly, the concept of a maximum droplet volume will be examined, then the influence of the sharpness of the source, as defined by cone angle, will be explored and finally, the relationship between the detached droplet volume and the general condition of the source will be discussed.

5.1. Estimates of a maximum droplet volume

The detached droplet volume predictions in Section 2.3 and the experimental results presented in Section 4.2 provide estimates of the maximum droplet volume that is possible from detachment from a surface or orifice. This will occur when the surface is flat and is independent of how the blood has accumulated on that surface. It is beneficial to explore this concept in more detail, including alternative methods of calculation, in order to better understand the factors that most affect the value of this quantity and its sensitivity to them.

Using the pendent drop profile method, the threshold minimum orifice radius has been calculated for the formation of the maximum droplet volume for a liquid which completely wets a solid surface ($\theta = 0°$) [32]. Using this formula, with the capillary length for horse blood, gives this radius as:

$$R_{th} = 2.2766a^* = 2.2766 \times 3.598 \times 10^{-3} = 8.19 \text{ mm}$$

The consequent pendent droplet volume is then given by Ref. [32]:

$$V_p = 6.7045 \times a^{*3} = 6.7045 \times (3.598 \times 10^{-3})^3 = 312.3 \quad \mu\text{L}$$

Hence, the detached droplet volume, calculated using the algorithm described earlier to generate the H–B correction factor, is given by:

$$V = V_p \times F\left(\frac{R}{V^{1/3}}\right) = 312.3 \times 0.5879 = 183.6 \quad \mu\text{L}$$

This is equivalent to a detached droplet diameter of 7.052 mm.

For comparison with experimental values where the contact angle is not zero, an adjustment to this approach needs to be included. A table of correction factors to the pendent droplet volume, by contact angle, has been theoretically derived [33]. For this present work where a contact angle of 25° was measured for a droplet formed on a flat, wetted brass surface, the consequent detached droplet volume may be calculated, using the appropriate factor, as:

$$V = (5.5080/6.7045) \times 183.6 = 150.8 \quad \mu\text{L}$$

Using these factors [33], predicted maximum detached droplet volumes as a function of contact angle may be calculated and are shown graphically in Fig. 3. This demonstrates how crucial is the wetting behaviour of the blood on the surface in determining the volume of the detached droplet as the volume decreases quite rapidly once the angle is above 20° or so. Moreover, the carefully controlled and stable conditions assumed in the theoretical models and, to some extent, achievable in laboratory experiments will not be sustained in case-work scenarios, with the result that droplet volumes will be commonly much lower than these predictions.

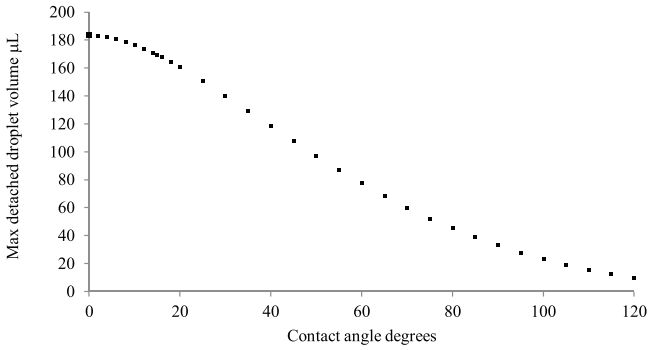

Fig. 3. Maximum detached droplet volume for horse blood as a function of contact angle using data from reference [33].

In contrast, previous work on droplet formation on conical tips [34,35] assumed 'completely wetting liquids' — that is, zero contact angle. The data needed to calculate the detached droplet volumes were extracted from the graphs presented in that paper [34] rather than from tabulated values and so any outcomes from this will be subject to further uncertainty. Despite this limitation, droplet volumes for horse blood have been calculated for each of the cone angles used in this current work and are given in Table 3. The contact angle correction factors [33] have been applied to these volumes and these estimates are also presented in this table together with the mean experimental values from the results presented in Section 4.2. For zero contact angle, the maximum detached droplet volume is 191 μL, decreasing to 157 μL under the experimental conditions measured here.

Finally, the maximum droplet volume may also be estimated using the approximation of Campbell [26] applied to the horse blood used here. The corresponding droplet diameter is given by Eq. (4), incorporating the value of the capillary length for horse blood derived earlier.

$$d = 2^{2/3}\sqrt{\frac{3\gamma}{\rho g}} = 1.944 \times a^* = 7.00\text{mm}$$

This is equivalent to a droplet volume of 179 μL.

Table 4 summarises all these estimates of the maximum droplet volume together with the average for the experimental results described here (final row in Table 3). There is a fair level of consistency across the different approaches for zero contact angle while for two of those the application of the contact angle

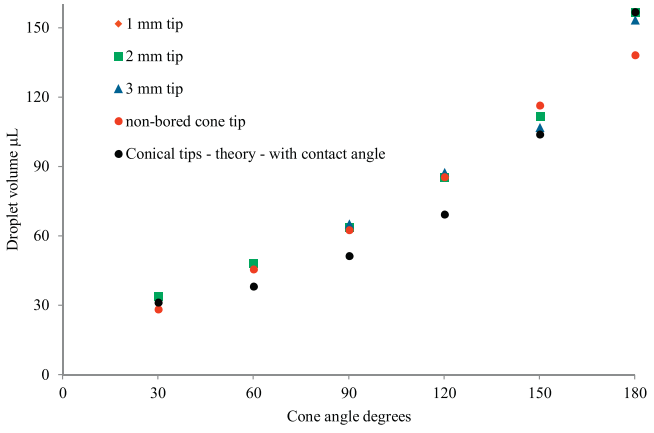

Fig. 4. Detached droplet volume as a function of cone angle for wetted tips.

Table 3
Detached droplet volumes for conical tips; theory and experiment.

Cone tip angle degrees	Detached droplet volume V μL					Expt[al] contact angle degrees	Theoretical estimates of detached droplet volume [34,33] V μL	
	Cone tip type							
	1 mm orifice	2 mm orifice	3 mm orifice	Solid cone	Mean expt[al] droplet volume μL		For zero contact angle	With contact angle correction
30	30.5	34.1	–	28.4	31.0	$(5)_{est}$	31.6	31.3
60	47.6	48.2	–	45.6	47.1	10	39.7	38.3
90	–	63.5	65.3	62.5	63.8	16	56.2	51.4
120	–	85.3	87.4	85.5	86.1	19	78.4	69.4
150	–	111	106	116	111	22	122	104
180	–	156	153	138	149	25	191	157

Table 4
Estimates of the maximum droplet volume for defibrinated horse blood.

Contact angle degrees	Source	Maximum droplet volume V μL
Zero	Drop shape theory [32]	184
	Drop weight theory [21,23]	205
	Drop weight theory + Campbell approx. [26]	179
	Drop shape theory; conical tips [34]	191
25°	Drop shape theory [33]	151
	Drop shape theory; conical tips [34]	157
	Experiment (this work)	149 ± 6

correction factor yields similar volumes, both of which are close to what has been measured experimentally, taken as the mean of the three results presented in Table 3.

Of course, all these droplet volumes relate to defibrinated horse blood. On the basis that these theoretical predictions have been validated by this experimental data, the equivalent maximum droplet volume for human blood, may also be calculated according to drop shape theory. Using the capillary length for human blood given in Section 2.1 and assuming the same contact angle, the maximum detached droplet volume is given by:

$$V = (5.5080/6.7045) \times 0.5879 \times 276.0 = 133.3 \quad \mu\text{L}$$

The difference in this value, from that for horse blood, reveals the relative sensitivity of this quantity to the ratio γ/ρ for the blood.

Within the bloodstain pattern analysis discipline, the concept of a 'standard', 'normal' or 'typical' droplet volume has been used, though its meaning has not been clearly defined. A value of 50 μL is commonly assigned to this quantity. Originally, it appears to have related to an average droplet volume released from typical body wounds under passive conditions but became conflated with the idea of this representing a maximum as, despite being an average, volumes very much larger than this occurred rarely in casework [38]. Fundamentally, as has been shown here, a maximum droplet volume is a valid quantity but in practice whether under laboratory or casework conditions, its magnitude, depends very much on the nature of the surface or orifice from which it is released so that its measurement in real circumstances will yield values that are normally very much less than that predicted theoretically for an ideal system. Hence, in that sense, for a given set of circumstances there will be a typical droplet volume but that quantity will not be transferable in any meaningful way to any, quite different scenario.

5.2. Droplet volumes from conical tips

The experimental detached droplet volumes from all wetted conical tips, together with the theoretical estimates calculated using published data [34], are presented in Table 3 and graphically as a function of cone angle, in Fig. 4. The contact angle correction factors were assigned using the experimentally measured angles given in Table 3. The contact angle for the 30° tip could not be determined experimentally so an estimated value by extrapolation was adopted here. It should be noted that the table of published factors [33] apply to droplets formed on flat surfaces and their transfer to conical surfaces should be regarded as an approximation. Nevertheless, this table shows good agreement amongst the results for the different orifice sizes and the non-bored tips which suggest that, within the range examined here, the detached droplet volume is independent of whether the source of the blood droplet is an orifice or a solid tip and, if the former, is also independent of the orifice size. There is more scatter for the two largest cone angles which may be attributed to the difficulties in experimentally delivering the blood to the tip under those conditions. The theoretical values appear to under-estimate the experimental volumes to some extent for the 90° and 120° angles, though elsewhere the agreement is reasonable. The relationship between volume and angle forms a smooth curve which, if extrapolated below 30°, suggests a limiting value of between 20–30 μL for a detached droplet from a conical tip as the cone angle sharpens towards zero. This particular conclusion deserves further investigation.

5.3. Droplet size and source condition

It is useful to discuss the range of droplet sizes that have been found experimentally in this work and their relationship to the conditions under which they were formed. This may provide some underpinning scientific basis to the interpretation of droplets and stains found in casework circumstances. Within the range of sources examined here, there are clearly maximum and minimum droplet volumes released and these will depend very much on the degree of wetting of the source by the blood. The relevant experimental values are summarised in Table 5 where mean values are taken across the relevant individual measurements presented earlier.

These results suggest that for those cones with the more acute angles, the range of potential droplet volumes falls within a

Table 5
Summary of mean experimental detached droplet volumes from non-wetted and wetted tips.

Cone tip angle degrees	Orifice diameter mm	Droplet volume (non-wetted) V μL	Droplet volume (wetted)[a] V μL	Droplet diameter (wetted)[a] mm
30	1	16	31	3.9
	2	30		
60	1	16	47	4.5
	2	30		
90	2	30	64	5.0
	3	43		
120	2	30	86	5.5
	3	43		
150	2	30	111	6.0
	3	43		
180	2	30	149	6.6
	3	43		

[a] Including the result from the non-bored tip in this average.

narrower range and hence the degree of wetting of the source is less significant. In contrast, for much wider angles and approaching a flat surface, the range is much larger and much more dependent on the extent of wetting and source surface characteristics. Clearly there are larger orifice sizes, not investigated in this study, which will yield larger droplet volumes under non-wetted conditions but these may be predicted using Eq. (3). For any cone angle, once an orifice is sufficiently large that the pendent drop pins to its circumference, the detached droplet volume will be defined by the orifice diameter and not by the cone angle. The maximum detached droplet volume from any sufficiently large orifice remains at around 150 μL under ideal conditions.

With casework examples in mind, interest is focused on the results in the final two columns of Table 5. Comparison of a weapon tip with the closest conical equivalent given here would allow estimation of the volume and diameter of passively detached droplets under gravity, taking into account the degree of wetting of the weapon by the blood. Further work on tips with different geometric shapes would provide additional reference data for such comparisons.

It is pertinent to compare these results with published droplet sizes released under gravity from real and model weapon tips of differing curvature, using porcine blood [17]. The difference in the γ/ρ factor means that droplet volumes will be expected to be around 5% and diameters around 1.5% larger for horse than for porcine blood. Direct comparison is not possible with the conical tips used here but some general comments may be made. Across all types of tips investigated, the detached droplet volumes were in the range 37.4–121.8 μL with the larger volumes being released from surfaces with larger radii of curvature [17]. This corresponds very well to the results shown for wetted conical tips in Table 5 where volumes from 31 to 149 μL were found. Surface roughness effects were found not to be strong factor in relation to detached droplet volume and, although contact angle effects are discussed, no detail on this is provided for the experimentally measured droplets nor is the degree of pre-wetting of the surface discussed specifically [17].

6. Detached droplets from swing-cast-off

Having discussed the passive detachment of blood droplets under gravity, it is of interest to extend these ideas to the active detachment of droplets under other forces, most notably the centrifugal force generated during swing-cast off. Here, simple theoretical approaches to cast-off will be presented and then applied to some recently published data. It is believed this is the first time that a mathematical model of swing cast-off has been applied to the quantitative prediction of the sizes of ejected blood droplets. For motion in a horizontal swing plane, any contribution from gravity may be neglected while for a vertical swing plane the gravitational force will make a contribution depending on the point in the motion at which the droplets are ejected. Nevertheless, in most practical circumstances the gravitational force is much smaller than that from centrifugal action so will not be considered here. Experimental studies have been published where a mechanical device designed to operate in a vertical plane has been used to generate droplets under controlled conditions [12,16] and data from these will be used to test mathematical models for the ejection mechanism.

6.1. Review of swing cast-off research

The fundamental action of ejecting liquid droplets by centrifugal force generated by a rotation mechanism is the basis of many applications where dispersal of 'atomised' liquid is required; for example, the action of agricultural sprays [39] and in chemical and food manufacture. There is a significant literature around this topic which facilitates our understanding of the creation of blood spatter droplets by swing cast-off action. It is not the present purpose to review that literature but simply to refer to some points that are most relevant to the current analysis. Depending of the flow rate of the liquid along the rotating arm, there are three types of disintegration that can occur. At the lowest flow rates, droplets are ejected directly from the arm then, as the flow increases, liquid ligaments may be formed [18]. A transition region may be identified where features of both these mechanisms occur [39]. At the highest flow rates the liquid is ejected as sheets [39]. Both the ligaments and sheets disintegrate further once they travel away from the rotation mechanism and droplets may then be formed.

In recent years there has been some interest in producing swing cast-off droplets under carefully controlled experimental conditions. A system for generating cast-off blood droplets has been described [16] which is based on an aluminium disc of radius 0.3 m rotating in a vertical plane with narrow radial grooves milled on one face. These were intended to guide the blood as it flows outwards to be ejected at the disc perimeter. Subsequent trajectories for droplets produced by this device at a range of tangential velocities have been measured and some additional quantitative data on droplet diameters and shape oscillations were obtained using high-speed photography [12]. Images from these studies show that, under these experimental conditions, the blood droplets may be released by disintegration of a ligament generated by the centrifugal force on blood within the channels [16]. Examples of the measurement of cast-off droplet diameters produced under a range of rotational speeds have been published from work using this system but these were not interpreted using any quantitative model. A simpler mechanical device for this

purpose has been used to generate cast-off stain patterns and these have been analysed in terms of stain density, aspect ratio and hence impact angle, again using high speed photography [14]. More recently, cast-off patterns have been produced from mechanically driven weapons and the trajectories carefully interpreted to gain a better idea of how the pattern is formed from droplets ejected at different points across the swing arc [18]. This shows one example of an image of ligament disintegration from a baseball bat tip travelling close to 15 ms^{-1} but no specific examples of droplet sizes are provided from this work.

6.2. Physical principles of swing cast-off

For swing cast-off action, the key modification to the model for passive release of blood under gravity is now that the gravitational force mg is replaced by the centrifugal force mv^2/L or the equivalent $m\omega^2 L$ where v is the linear (tangential) velocity at the point of detachment and ω is the angular velocity of the swing action; L is the radius of the circular rotational path. This centrifugal force F_c is generated by the torque applied to the weapon.

It is important to note that for passive dripping under gravity the force causing detachment of a droplet is the same at all points across the system. For the centrifugal force however, the magnitude increases linearly with distance along the rotating arm. Hence, with sufficient blood mass, it will usually be the case that this force is different across the blood mass which leads to it expanding as well as travelling outward along the radial direction.

If a droplet is formed statically on the weapon then the motion on leaving the weapon will be tangential to the point of ejection. However, if there is significant blood and there is motion of the blood mass radially along the weapon prior to droplet ejection, then the initial trajectory will not be purely tangential but will be the combination of the tangential speed with any radial velocity component along the weapon itself, though that is likely to be small compared to the tangential component. For droplets released by ligament disintegration, the path followed may be more complex depending on the motion of the ligament itself and the point at which the droplet detaches. Images of droplet formation have been published [12,16,18,39].

For a manufactured device, such as a rotary atomiser, which produces droplets from a continuous liquid flow, a fluid dynamics analysis has been used to derive expressions for ligament formation and the droplet diameters released under different conditions [39]. However, this approach cannot be directly applied to blood droplets formed under swing cast-off conditions from a weapon so more basic approaches are needed to estimate droplet size here. Two models will be considered: the first where the droplet is release from an orifice or similar structure on the rotating surface and another, more appropriate to release from a ligament, where the droplet is formed directly from the blood mass itself.

Replacing the gravitational force mg in the model for droplet formation from an orifice as described in Section 2.1 (Eq. (3)) leads to:

$$V = \pi\left(\frac{2\gamma L}{\rho v^2}\right) RF\left(\frac{R}{V^{1/3}}\right) \tag{8}$$

The capillary length a^* is now no longer a constant so it is more convenient to express the formula as shown here. This expression implies that higher velocities will result in the formation of smaller blood droplets.

This result may be expected to apply where a droplet is released after being pinned to some orifice or similar physical feature under radius-limited conditions on the rotating weapon. For the experimental system described previously [16] this would be the 1 mm by 1 mm grooves cut radially on the rotating disc where the magnitude of the surface tension force will depend on the contact length of the blood around the end of the groove on the disc circumference.

An alternative, yet quite simple model that does not directly relate to the dimension of any feature on the weapon has been described in the context of the disintegration of liquids – 'atomisation' – by means of a rotating cup [40]. This approach is similar to Campbell's method [26] for determining the maximum droplet volume released from a flat surface which was discussed in Section 2.1. The droplet separates from the bulging of blood on the weapon where there is no pinning to any feature on the weapon. Given that formation of a blood ligament is one instance of this effect, it is likely that this model is more appropriate for droplets released from a fragmenting ligament. Hence, the condition for separation is given by equating the centrifugal force to the surface tension around the contact length between the emerging droplet on the bulging blood mass which is assumed to be equal to the detaching droplet circumference:

$$\frac{mv^2}{L} = \pi\gamma d$$

Writing the mass in terms of the density and volume of the droplet and re-arranging for d gives:

$$d = \sqrt{\frac{6\gamma L1}{\rho\ v}} \tag{9}$$

This result (Eq. (9)), though very much an order of magnitude model, implies that droplet diameter d and linear velocity v are in inverse proportion. In contrast, the first model for droplet release, governed by some orifice or structural feature of defined size on the weapon (Eq. (8)), suggests a basic relationship governed by:

$$d \propto\sim v^{-2/3}$$

This is modified to some small extent by the H–B correction factor F.

6.3. Testing models of droplet release

Using published data generated by the rotating disc system [12,16], these two models have been used to calculate theoretical estimates for the diameters of blood droplets released under those experimental conditions. These are then compared to the experimental values in Table 6. As porcine blood was used in these experiments, appropriate published density and surface tension values [12] were adopted in these calculations, using $\gamma/\rho = 0.0638/1054 = 6.053 \times 10^{-5}$ $m^{-3}s^{-2}$. Although values for these parameters from two sources are quoted in [12], both give similar results for this ratio. It has been assumed here that the channels in the disc are fully filled with blood and the surface tension line at the edge of the disc was approximated to a circle of radius 0.5 mm for convenience.

These results shows that, although they are of similar magnitudes, all the theoretical values are larger than those found experimentally and indeed, if this comparison was done on a droplet volume basis, a far larger discrepancy would be evident between theory and experiment. For lower swing velocities the predictions of Eq. (8) appear better while for the highest velocities, Eq. (9) provides slightly closer agreement to experiment. This can be rationalised by considering that at these lowest rotational speeds the blood movement along the channel in the rotating disc will be lower and so direct detachment of droplets from the edge of the disc is more likely. On the other hand at high speeds the more rapid movement of blood along the channel will produce ligaments

Table 6
Experimental values and theoretical predictions for cast-off droplet diameters.

Experiment		Reference	Theory	
Tangential velocity v ms^{-1}	Droplet diameter d mm		d (Eq. (8)) mm	d (Eq. (9)) mm
4	1.46	[12]	1.7	2.6
6	0.9	[16]	1.3	1.7
10	0.6	[16]	0.87	1.0
15	0.48	[12]	0.66	0.70
20	0.26	[16]	0.56	0.52
30	0.18	[16]	0.41	0.35

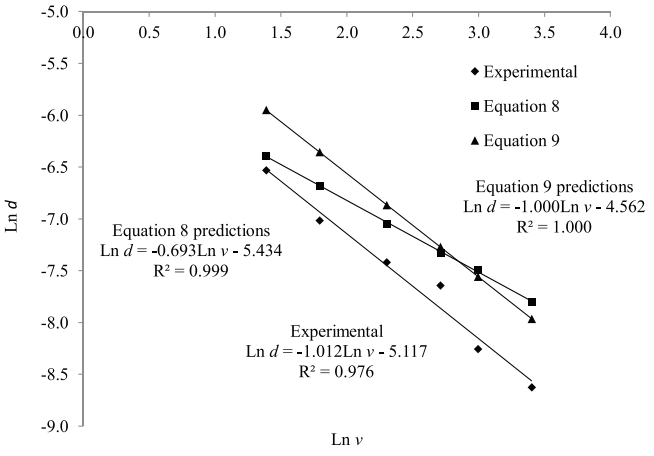

Fig. 5. Plot of Ln d versus Ln v for published swing cast-off droplet data and for theoretical models.

from which droplets will be released, the size of which will not be directly related to the channel size. For the first model, the droplet volumes can be reduced to some extent by assuming the channels are only partly filled with blood but this factor is unknown. The second model assumes the surface tension force depends directly on the droplet diameter whereas we would expect some necking to occur on the ligament leading to a smaller detached droplet, as the retaining force would be less. Neither model considers the rate of droplet release or the blood flow rate along the channels. These factors may at least partly explain the discrepancies in Table 6.

It is of interest to review the experimental data on the basis of a power law relationship between v and d and to compare that with the dependency between these quantities describe earlier for these two models. Any power law relationship between d and v is most clearly determined by a graph of Ln d vs Ln v. These are presented in Fig. 5. The gradient of the equation for the linear regression line through the experimental data points is −1.01 which clearly shows that, across this range of speeds, the dependency of these data is most closely modelled by Eq. (9). This is consistent with the observations of droplet release from ligaments reported in these experiments [16]. In contrast, the calculated power for Eq. (8) was found to be −0.69 which is very close to the dependency of −2/3 before application of the H–B correction factor. An empirical adjustment to Eq. (9) which fairly accurately predicts these experimental data, may be made on the basis of the regression line through the experimental data which yields (for d in m):

$$d = \frac{0.0060}{v} \tag{10}$$

Further development of theoretical models for swing-cast off must await more detailed experimental data, in particular where differing methods for releasing the blood from the rotating disc and specific photographic data on the mechanism of release for droplets under differing tangential velocities, have been investigated. Further key factors are the flow rate along the channels and the rate of release of droplets, given these are known to relate to the droplet size and again time-lapsed photographic data should enable examination of that issue.

7. Conclusions

These theoretical and experimental investigations into the formation and release of blood droplets from orifices and surfaces have provided several significant conclusions that potentially enhance the interpretation of blood evidence from weapon tips encountered in casework. For passive release under gravity, theoretical models based on the pendent drop weight and shape methods have been shown to predict detached droplet volumes from non-wetted orifices, under radius-limited conditions, to a good degree of accuracy. When the conical tips are pre-wetted with blood the contact angle made by the pendent droplet with the tip surface becomes a crucial factor in determining the detached droplet volume. This volume is found to be independent of whether the blood flows from an orifice on to the tip or over the conical tip surface itself in the case of un-bored nozzles. Here the droplets are held on to the tip surface by the surface tension force and are said to be angle-limited. Detached droplet volumes are predicted fairly well by applying the contact angle correction factors originally derived for flat surfaces [33] to these conical tips. Droplet volume increases with cone angle and, for a flat horizontal surface, the detached droplet volume corresponds very well to theoretical predictions with a value of around 150 μL for the experimental conditions in this work. Furthermore, these data suggest that for the sharpest conical tips a lower droplet volume of around 20–30 μL is likely. The degree of wetting of the weapon tip with blood and the wettability of the surface itself, as well as the degree of sharpness of the tip, are the key factors in determining the volume of released blood droplets. These results provide quantitative data and theoretical models to underpin these conclusions. Although this work was carried out using defibrinated horse blood, all the numerical results may be converted to equivalent values for human blood using the appropriate γ/ρ factor.

The mathematical models used to predict passive release have been modified to describe the active release of blood droplets under conditions of swing cast-off by replacing the gravitational acceleration with that arising from the centrifugal force. Using published data, derived from a device designed to physically simulate the cast-off process [12,16], it has been shown that both the mathematical models considered here provide estimates of detached droplet diameters that are in order of magnitude agreement with those found experimentally. However, the model which is based on a mechanism whereby the detaching droplet is release directly from a blood mass on the weapon, shows excellent functional agreement – $d \propto\sim v^{-1}$ – with the published data. This may be indicative of blood ligament formation prior to the droplet release itself, as was observed experimentally [16]. Nevertheless, further experimental and theoretical work remains to be done to refine our understanding of this aspect of blood droplet formation and release.

Declarations of interest

None.

CRediT authorship contribution statement

Craig D. Adam: Conceptualization, Data curation, Formal analysis, Investigation, Methodology, Project administration, Resources, Software, Validation, Visualization, Writing - original draft, Writing - review & editing.

Acknowledgements

This research did not receive any specific grant from funding agencies in the public, commercial, or not-for-profit sectors.

References

[1] S. Chandra, C.T. Avedisian, On the collision of a droplet with a solid surface, Proc. R. Soc. Lond. A 432 (1991) 13–41, doi:http://dx.doi.org/10.1098/rspa.1991.0002.
[2] M. Pasandideh-Fard, Y.M. Qiao, S. Chandra, J. Mostaghimi, Capillary effects during impact on a solid surface, Phys. Fluids 8 (3) (1996) 650–659, doi:http://dx.doi.org/10.1063/1.868850.
[3] L. Hulse-Smith, N.Z. Mehdizadeh, S. Chandra, Deducing drop size and impact velocity from circular bloodstains, J. Forensic Sci. 50 (1) (2005) 1–10, doi:http://dx.doi.org/10.1520/JFS2003224.
[4] N.Z. Mehdizadeh, S. Chandra, J. Mostaghimi, Formation of fingers around the edges of a drop hitting a metal plate with high velocity, J. Fluid Mech. 510 (2004) 353–373, doi:http://dx.doi.org/10.1017/S0022112004009310.
[5] L. Hulse-Smith, M. Illes, A blind trial evaluation of a crime scene methodology for deducing impact velocity and droplet size from circular bloodstains, J. Forensic Sci. 52 (1) (2007) 65–69, doi:http://dx.doi.org/10.1111/j.1556-4029.2006.00298.x.
[6] C.D. Adam, Fundamental studies of bloodstain formation and characteristics, Forensic Sci. Int. 219 (1) (2012) 76–87, doi:http://dx.doi.org/10.1016/j.forsciint.2011.12.002.
[7] D. Attinger, C. Moore, A. Donaldson, A. Jafari, H.A. Stone, Fluid dynamics topics in blood stain pattern analysis: comparative review and research opportunities, Forensic Sci. Int. 231 (1–3) (2013) 375–396, doi:http://dx.doi.org/10.1016/j.forsciint.2013.04.018.
[8] C.D. Adam, Experimental and theoretical studies of the spreading of bloodstains on painted surfaces, Forensic Sci. Int. 229 (2013) 66–74, doi:http://dx.doi.org/10.1016/j.forsciint.2013.03.044.
[9] N. Laan, K.G. de Bruin, D. Bartolo, C. Josserand, D. Bonn, Maximum diameter of impacting liquid droplets, Phys. Rev. Appl. 2 (4) (2014)044018, doi:http://dx.doi.org/10.1103/PhysRevApplied.2.044018.
[10] C. Knock, M. Davison, Predicting the position of the source of blood stains for angled impacts, J. Forensic Sci. 52 (5) (2007) 1044–1049, doi:http://dx.doi.org/10.1111/j.1556-4029.2007.00505.x.
[11] N. Laan, K.G. de Bruin, D. Slenter, J. Wilhelm, M. Jermy, D. Bonn, Bloodstain pattern analysis: implementation of a fluid dynamic model for position determination of victims, Sci. Rep. 5 (2015) 11461, doi:http://dx.doi.org/10.1038/srep11461.
[12] N. Kabaliuk, M.C. Jermy, E.M.P. Williams, T.L. Laber, M.C. Taylor, Experimental validation of a numerical model for predicting the trajectory of blood drops in typical crime scene conditions, including droplet deformation and breakup, with a study of the effect of indoor air currents and wind on typical spatter drop trajectories, Forensic Sci. Int. 245 (2014) 107–120, doi:http://dx.doi.org/10.1016/j.forsciint.2014.10.020.
[13] C. Flight, M. Jones, K.N. Ballantyne, Determination of the maximum distance blood spatter travels from a vertical impact, Forensic Sci. Int. 293 (2018) 27–36, doi:http://dx.doi.org/10.1016/j.forsciint.2018.10.015.
[14] S.N. Kunz, J. Adamec, C. Grove, Analyzing the dynamics and morphology of cast-off pattern at different speed levels using high-speed digital video imaging, J. Forensic Sci. 62 (2) (2017) 428–434, doi:http://dx.doi.org/10.1111/1556-4029.13299.
[15] D. Attinger, P.M. Comiskey, A.L. Yarin, K. De Brabanter, Determining the region of origin of blood spatter patterns considering fluid dynamics and statistical uncertainties, Forensic Sci. Int. 298 (2019) 323–331, doi:http://dx.doi.org/10.1016/j.forsciint.2019.02.003.
[16] E. Williams, M. Taylor, The development and construction of a motorized blood droplet generation device (BDGD) for detailed analysis of blood droplet dynamics, J. Bloodstain Pattern Anal. 29 (1) (2013) 14–29.
[17] N. Kabaliuk, M.C. Jermy, K. Morison, T. Stotesbury, M.C. Taylor, E.M.P. Williams, Blood drop size in passive dripping from weapons, Forensic Sci. Int. 228 (1–3) (2013) 75–82, doi:http://dx.doi.org/10.1016/j.forsciint.2013.02.023.
[18] E.M.P. Williams, E.S. Graham, M.C. Jermy, D.C. Kieser, M.C. Taylor, The dynamics of blood drop release from swinging objects in the creation of cast-off bloodstain patterns, J. Forensic Sci. 64 (2) (2019) 413–421, doi:http://dx.doi.org/10.1111/1556-4029.13855.
[19] S. Middleman, Modeling Axisymmetric Flows, Dynamics of Films, Jets and Drops, Academic Press, San Diego, 1995.
[20] Lord Rayleigh, Investigations in capillarity, Philos. Mag. 48 (1899) 321–337, doi:http://dx.doi.org/10.1080/14786449908621342.
[21] W.D. Harkins, F.E.J. Brown, The determination of surface tension and the weight of falling drops, Am. Chem. Soc. 4 (1919) 499–524, doi:http://dx.doi.org/10.1021/ja01461a003.
[22] Z.Q. Zhang, Y. Mori, Formulation of the Harkins-Brown correction factor for drop-volume description, Ind. Eng. Chem. Res. 32 (1993) 2950–2952, doi:http://dx.doi.org/10.1021/ie00023a070.
[23] J.C. Earnshaw, E.G. Johnson, B.J. Carroll, P.J. Doyle, The drop volume method for interfacial tension determination: an error analysis, J. Colloid Interface Sci. 177 (1996) 150–155, doi:http://dx.doi.org/10.1006/jcis.1996.0015.
[24] B.-B. Lee, P. Ravindra, E.-S. Chan, A critical review: surface and interfacial tension measurement by the drop weight method, Chem. Eng. Commun. 195 (2008) 889–924, doi:http://dx.doi.org/10.1080/00986440801905056.
[25] O.E. Yildirim, Q. Xu, O.A. Basaran, Analysis of the drop weight method, Phys. Fluids 17 (2005)062107, doi:http://dx.doi.org/10.1063/1.1938227.
[26] J. Campbell, Surface tension measurement by the drop weight method, J. Phys. D: Appl. Phys. 3 (1970) 1499–1504, doi:http://dx.doi.org/10.1088/0022-3727/3/10/420.
[27] B.B. Freud, W.D. Harkins, The shapes of drops and the determination of surface tension, J. Phys. Chem. 33 (8) (1929) 1217–1234, doi:http://dx.doi.org/10.1021/j150302a012.
[28] R.C. Brown, H. McCormick, A new drop-weight method for the comparison of surface tensions, Philos. Mag. 39 (1948) 420–428, doi:http://dx.doi.org/10.1080/14786444808521691.
[29] C.E. Stauffer, The measurement of surface tension by the pendant drop technique, J. Phys. Chem. 69 (6) (1965) 1933–1938, doi:http://dx.doi.org/10.1021/j100890a024.
[30] J.F. Padday, The profiles of axially symmetric menisci, Philos. Trans. R. Soc. Lond. A 269 (1197) (1971) 265–293, doi:http://dx.doi.org/10.1098/rsta.1971.0031.
[31] J.F. Padday, A.R. Pitt, The stability of axisymmetric menisci, Philos. Trans. R. Soc. Lond. A 275 (1253) (1973) 489–528, doi:http://dx.doi.org/10.1098/rsta.1973.0113.
[32] E.A. Boucher, M.J.B. Evans, Pendent drop profiles and related capillary phenomena, Proc. R. Soc. Lond. A 346 (1646) (1975) 349–374, doi:http://dx.doi.org/10.1098/rspa.1975.0180.
[33] E.A. Boucher, M.J.B. Evans, H.J. Kent, Capillary phenomena II: equilibrium and stability of rotationally symmetric fluid bodies, Proc. R. Soc. Lond. A 349 (1656) (1976) 81–100, doi:http://dx.doi.org/10.1098/rspa.1976.0061.
[34] S.R. Babu, Analysis of drop formation at conical tips: 1 theory, J. Colloid Interface Sci. 116 (2) (1987) 350–358, doi:http://dx.doi.org/10.1016/0021-9797(87)90131-7.
[35] S.R. Babu, Analysis of drop formation at conical tips: 2 experimental, J. Colloid Interface Sci. 116 (2) (1987) 359–372, doi:http://dx.doi.org/10.1016/0021-9797(87)90132-9.
[36] B.A.J. Larkin, C.E. Banks, Exploring the applicability of equine blood to bloodstain pattern analysis, Med. Sci. Law 56 (3) (2016) 190–199, doi:http://dx.doi.org/10.1177/0025802414542456.
[37] G.W.C. Kaye, T.H. Laby, Tables of Physical and Chemical Constants, 16th ed., Longman, Harlow, 1995.
[38] S.H. James, P.E. Kish, T.P. Sutton, Principles of Bloodstain Pattern Analysis — Theory and Practice, CRC Press, Boca Raton, 2005.
[39] A.R. Frost, Rotary atomisation in the ligament formation mode, J. Agric. Eng. Res. 26 (1981) 63–78, doi:http://dx.doi.org/10.1016/0021-8634(81)90127-X.
[40] J. Liu, Q. Yu, Q. Guo, Experimental investigation of liquid disintegration by rotary cups, Chem. Eng. Sci. 73 (2012) 44–50, doi:http://dx.doi.org/10.1016/j.ces.2012.01.010.